Advances in Nano Research, *Vol. 18, No. 5 (2025) 419-432*
https://doi.org/10.12989/anr.2025.18.5.419

Exercise-induced changes in protein tissue stability in athletes via biomechanical analysis using size-dependent mechanical models

Chaofan Chen[1,4], Xiangzi Xiao[3,4], Liang Chen[*2,4], Mostafa Habibi[5,6,7], Ameni Brahmia[8] and Xiaodao Chen[9]

[1]*College of Arts & Physical Education, Gangneung-Wonju National University, Gangneung-si 25457, Gangwon-do, Korea*
[2]*Sports Department, CHANG'AN UNIVERSITY, Xi'an 710064, Shaanxi, China*
[3]*Department of Education, Taylor's University, Jalan Taylor's,47500 Subang Jaya, Selangor Malaysia*
[4]*Sports College, Henan Untversity, Kaifeng 475000, Henan, China*
[5]*Universidad UTE, Facultad de Arquitectura y Urbanismo, Calle Rumipamba S/N y Bourgeois, Quito 170147, Ecuador*
[6]*Department of Biomaterials, Saveetha Dental College and Hospital, Saveetha Institute of Medical and Technical Sciences, Chennai 600 077, India*
[7]*Institute of Research and Development, Duy Tan University, Da Nang 550000, Viet Nam*
[8]*Department of Chemistry, College of Science, King Khalid University, P.O. Box 9004, 61413 Abha, Saudi Arabia*
[9]*Institute Sciences and Design of AL-Kharj, Dubai, United Arab Emirates*

(*Received September 17, 2022, Revised Aprill 7, 2025, Accepted April 9, 2025*)

Abstract. Protein stability has been recognized as a critical factor influencing athletic performance, recovery, and injury prevention during physical exercise. Despite widespread recognition, the mechanisms by which exercise influences the stability of protein tissues and fibers remain incompletely understood. This study uses complex mechanical theories and numerical simulations to investigate how exercise impacts protein stability. Size-dependent mechanical models are employed to analyze the small-scale behavior of protein tissues under exercise-induced stress, including strain rate, tissue microstructure, and exercise intensity. Numerical approaches are used to simulate proteins' dynamic behavior, offering insights into their deformation and failure processes under a wide range of situations. The results demonstrate that exercise substantially influences protein stability, with significant variations depending on the kind and intensity of the physical activity. These findings provide novel insights into the importance of protein stability in athletic performance and recovery, highlighting practical implications for training optimization, injury prevention, and broader applications in sports science. This study emphasizes the importance of protein stability for exercise and athletic performance by integrating biomechanics and sports science.
Keywords: athletic performance; biomechanical analysis; exercise-induced changes; numerical simulations; protein stability; size-dependent models

1. Introduction

Protein stability is fundamental to athletic performance, influencing the structural integrity of muscle fibers, tendons, and ligaments during dynamic physical activities. Recent developments in biomechanical modeling, particularly in relation to sports equipment and composite structures, underscore the importance of material stability when subjected to mechanical stress (Wang *et al*. 2023a, c, Wu *et al*. 2023). Studies on graphene-reinforced composites and functionally graded materials have demonstrated the influence of microscale heterogeneities on mechanical resilience, a concept applicable to protein tissues under exercise-induced loads. The behavior of protein fibers under strain resembles the responses seen in advanced sports structures, including viscoelastic panels and laminated nanoshells, where stability and deformation thresholds that depend on frequency influence performance outcomes. Athletic activities exert intricate mechanical stresses on biological tissues, such as cyclic loading, shear forces, and localized strain gradients, potentially destabilizing protein structures. This aligns with findings in research on sports equipment, including the dynamic stability analysis of composite curved pipes and the buckling resistance of functionally graded micro-tubes (Li *et al*. 2024b), where material failure is influenced by microscale interactions and load distribution. For instance, Wang *et al*. (2024a) highlighted the significance of nonuniform material properties in cylindrical beam structures. This principle is equally crucial for comprehending how exercise-induced stress gradients destabilize protein networks. In a similar vein, Zhu *et al*. (2024b) examined the hygrothermal effects on gymnastics beams, highlighting the relationship between environmental conditions and mechanical responses, a framework relevant to physiological environments during exercise.

Despite these parallels, previous studies on protein stability have primarily concentrated on biochemical or thermal factors (Man *et al*. 2024, Song *et al*. 2024), overlooking the biomechanical forces that are crucial to athletic performance. Traditional models, including those examining thermal stress in piezoelectric sports plates (Wang *et al*. 2024g) and electro-magneto-elastic diving boards (Wang *et al*. 2024d), do not possess the resolution

*Corresponding author, Ph.D.,
E-mail: blance968@126.com

ISSN: 2287-237X (Print), 2287-2388 (Online)

necessary to account for size-dependent protein dynamics. Recent research on sports equipment illustrates the significance of advanced mechanical theories. For example, Ma *et al*. (2024) utilized modified strain gradient theory to forecast static and dynamic responses in sandwich micro-plates, whereas Guo *et al*. (2024) implemented nonlocal strain gradient principles to examine electroelastic wave dispersion in nanosensors. These approaches underscore the need for scale-sensitive models to elucidate nanoscale protein behavior under athletic loads (Omidi *et al*. 2013, Mousavi *et al*. 2017, Shahabinejad *et al*. 2018). The incorporation of biomechanical principles into the analysis of protein stability is substantiated by research on sports structures, including the energy absorption of vibrating athlete performance plates (Wang *et al*. 2024e) and the dynamic stability of spinning cylindrical components (Zhang *et al*. 2024a). These studies demonstrate the correlation between mechanical instability thresholds and performance degradation, a crucial concept for connecting protein-level failures, such as fiber buckling or denaturation, to macro-scale athletic injuries. This study integrates methodologies from sports engineering, including AI-driven predictions of buckling in micro-tubes and computational stability analyses of gymnastic accessories, thereby connecting material science with exercise physiology and providing a new biomechanical perspective on protein stability.

Traditional models for assessing protein stability in athletic contexts typically depend on macroscale continuum mechanics or simplified thermal and biochemical frameworks, overlooking the size-dependent dynamics that are essential at the microscale of protein tissues (Huang *et al*. 2024b, Liu *et al*. 2024a, Wu *et al*. 2024a). Studies such as Li *et al*. (2024a), which utilized classical torsional analysis on metal-foam beams, and Wang *et al*. (2024f), which modeled foldable gymnastic accessories through eigenvalue approaches, illustrate the tendency of traditional methods to emphasize global structural responses rather than localized microscale interactions. In a similar vein, Zhao *et al*. (2024) utilized neuro-fuzzy systems to forecast springback in steel sheets, yet overlooked microstructural heterogeneities, a limitation akin to the neglect of protein fiber hierarchies in exercise physiology. These approaches do not adequately account for phenomena such as surface energy effects, nonlocal stress interactions, or strain gradients—elements that significantly influence nanoscale protein behavior under dynamic athletic loads (Liu *et al*. 2025a).

The limitations of classical models are apparent when their predictions are contrasted with advanced size-dependent frameworks (Wang *et al*. 2024h, j, k). For instance, Krysko *et al*. (2021) demonstrated that non-classical boundary conditions in concrete disks significantly modify stability thresholds, a result that cannot be replicated using conventional elasticity theory. Similarly, Shi *et al*. (2022) showed that electro-thermo-mechanical coupling in porous nanoshells leads to microscale stress concentrations that are not present in macroscale models. Discrepancies pose significant challenges for protein tissues, as hierarchical architectures, such as collagen fibrils and myofilaments, demonstrate deformation modes that are sensitive to scale. Research on sports equipment, as exemplified by Zhang *et al*. (2024b), where examination of foldable cylindrical shells reinforced which examined foldable cylindrical shells reinforced with graphene origami nanofillers, highlights the inadequacy of classical beam theories in accurately predicting buckling thresholds due to their disregard for nanoscale reinforcement effects, a limitation that also applies to protein fiber networks.

Recent advancements in materials science have adopted size-dependent theories, such as the application of hybrid nonlocal strain gradient models to curved nanopipes and microparameter-driven stress analysis of plates. In contrast, exercise physiology continues to rely on oversimplified paradigms. The use of folded nanostructures to enhance pole vault shells, as proven by Zhiqiang *et al*. (2024), emphasizes the importance of microscale design in load-bearing settings, nevertheless, comparable ideas are seldom used in protein tissues. In a similar line, the study of piezoelectric sandwich micro-panels and the modeling of higher-order foldability in shells demonstrate how sophisticated frameworks may solve localized instabilities, nonetheless, these breakthroughs remain neglected in biomechanical protein research.

Additionally, previous studies on protein stability have primarily concentrated on biochemical pathways (Man *et al*. 2024) or thermal stressors (Song *et al*. 2024), neglecting biomechanical factors. For instance, Xiao *et al*. (2024) examined imperfect bio-composite beams in environmental contexts but failed to consider mechanical strain-rate effects, whereas Wang *et al*. (2025) investigated nanoparticle -enhanced lubrication without establishing a connection between microscale interactions and macroscale wear resistance. This limited perspective creates significant deficiencies in comprehending how mechanical loads from exercise disrupt protein structures (Chen *et al*. 2025, Liu *et al*. 2025b, Wu *et al*. 2025). In contrast, the AI-driven stability prediction for nonuniform microstructures presented in study of Liang *et al*. (2024) and the multi-load analysis of origami-reinforced panels in research by Yu *et al*. (2024) demonstrate the predictive capabilities of scale-sensitive models, which are essential for mapping protein behavior under athletic stress.

Recent advances in size-dependent mechanical theories have transformed the study of microscale biomechanical systems, providing unparalleled accuracy in capturing the complex behaviors of protein tissues under exercise-induced stress (Chen *et al*. 2024, Liu *et al*. 2024b, Wu *et al*. 2024b). Unlike classical models, nonlocal elasticity and strain gradient theory clearly account for surface energy effects, nonlocal stress interactions, and material hetero-geneity, all of which are important considerations in understanding protein stability in sporting situations (Jining *et al*. 2025). For example, research on graphene origami (G-Ori) reinforced composites (Zhu *et al*. 2024a) and foldable nanostructures (Li *et al*. 2025) shows how size-dependent design principles improve load-bearing capacity and dynamic resilience in sports equipment, serving as a template for modeling hierarchical protein architectures.

The combination of these ideas with computer intelligence has increased their predictive potential. For example, Zisong and Habibi (2024) used neural-fuzzy systems and crystal plasticity to predict formability in steel

sheets, which is directly relevant to predicting protein fiber deformation under cyclic sports loads. Similarly, Jining *et al*. (2025) created a hybrid intelligent model for evaluating piezoelectric shells, resolving stress/strain patterns in deformable structures—an technique that may help explain how electro-thermo-mechanical interaction affects protein stability during exercise. These developments address macroscale model limits by resolving localized phenomena that traditional frameworks cannot see, such as stress concentrations at protein fiber junctions or strain-rate-dependent unfolding (Zhou *et al*. 2025).

Size-dependent models have already had a dramatic impact on sports engineering. Studies using stretchable-thickness graphene origami plates (Wang *et al*. 2024i) demonstrated how nanoscale reinforcements reduce dynamic instabilities in badminton equipment, replicating the effect of cross-linked protein networks in preventing exercise-induced weariness. Huang *et al*. (2024a) improved foldable golf club shells using eigenvalue-eigenvector approaches, showing how microscale geometry impacts macroscale performance, which is significant for understanding protein fibril alignment in tendons under mechanical load. These parallels show that size-dependent biomechanics in exercise physiology is neglected.

Emerging approaches, such as AI-driven stability prediction (Zhu *et al*. 2022) and multi-scale foldability modeling (Wang *et al*. 2024b), help to bridge the gap between material science and biological systems. For example, He *et al*. (2024) used modified non-classical theories to study composite concrete stability, which is applicable to forecasting protein network breakdowns under athletic stress gradients. Furthermore, Zhou *et al*. (2025) showed how carbon nanotube aggregation influences torsional responses in composite rods, providing insights into protein fiber interactions during high-intensity motions. By incorporating these advances, this research creates a biomechanical framework for quantifying exercise-induced protein instability and guiding training optimization and injury prevention measures.

This research tackles significant deficiencies in exercise physiology by utilizing size-dependent biomechanical models and sophisticated numerical simulations to elucidate the mechanisms behind exercise-induced protein instability. The objectives consist of three key components:

- To create a comprehensive biomechanical framework that measures protein stability under athletic loads, incorporating strain gradient theory and nonlocal elasticity principles to address nanoscale fiber interactions and macroscale tissue responses.
- The objective is to correlate exercise intensity, strain rate, and tissue microstructure with protein deformation thresholds through high-fidelity numerical simulations, while mapping dynamic failure modes across hierarchical architectures.
- The objective is to create practical guidelines aimed at enhancing training programs and preventing injuries, utilizing stability criteria that have been validated through athlete performance data and energy absorption metrics drawn from comparisons with sports equipment.

This work presents three significant contributions that are truly innovative:

- ✓ Initial implementation of size-dependent models derived from sports applications in the field of protein biomechanics: This study integrates methodologies from foldable nanostructures and graphene origami-reinforced composites, creating a connection between materials science and exercise physiology, and presenting a significant shift from traditional thermal and biochemical analyses.
- ✓ The integration of multiscale numerical frameworks involves the combination of nonlocal strain gradient theory and dynamic stability analysis. This approach addresses protein instability under cyclic loads, a feature lacking in classical continuum models.
- ✓ Application of translation to athletic performance: This study differentiates itself from previous research on static protein behavior by establishing a connection between microscale protein failures, such as fiber buckling, and macroscale injuries, including tendinopathies. This linkage is supported by stability criteria validated through athlete performance data and sports equipment mechanics.

This study establishes a biomechanics-to-practice pipeline that enhances theoretical understanding and provides coaches and athletes with evidence-based strategies to improve performance and longevity.

2. Mathematical formulation of protein tissue stability under exercise-induced loads

2.1 Linking protein tissue stability to mechanical engineering principles

Protein tissues, like muscle fibers and tendons, display hierarchical structures that support mechanical stresses during physical activity. These structures may be similarly represented as beam- or tube-like systems in mechanical engineering (Fig. 1), where external forces (e.g., exercise-induced stresses) and environmental conditions (e.g., heat variations) dictate their stability. Exercise produces mechanical loads (e.g., axial tension, shear, bending) and thermal stressors from elevated core body temperature, both of which destabilize protein tissues by causing microstructural deformations. To quantify these effects, we use size-dependent mechanical theories (e.g., modified couple stress theory) that include microscale material heterogeneity and inherent length-scale factors, which are essential for simulating biological tissues at the nanoscale.

2.2 Mechanical analogy: protein fibers as size-dependent beams/tubes

Protein fibers are represented as elastic cylindrical tubes within a viscoelastic matrix that simulates surrounding tissues (Fig. 2). The mechanical response of these fibers under loads induced by exercise is determined by:

- ✓ Geometric nonlinearity: Significant deformations resulting from repetitive athletic motions.
- ✓ Size-dependent effects: Nanoscale microstructural interactions (e.g., cross-linking, fibril alignment).

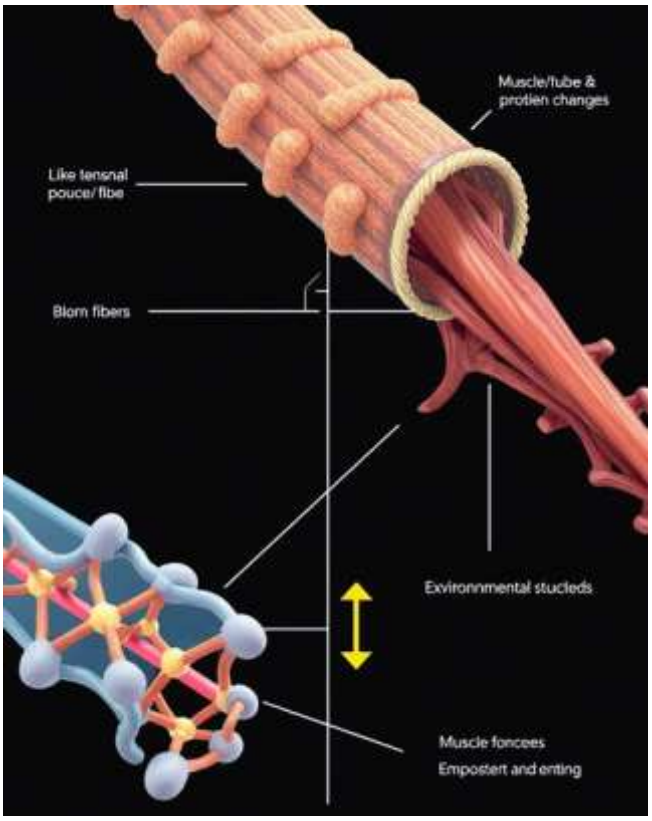

Fig. 1 Hierarchical structure of protein tissues and their mechanical engineering analogy

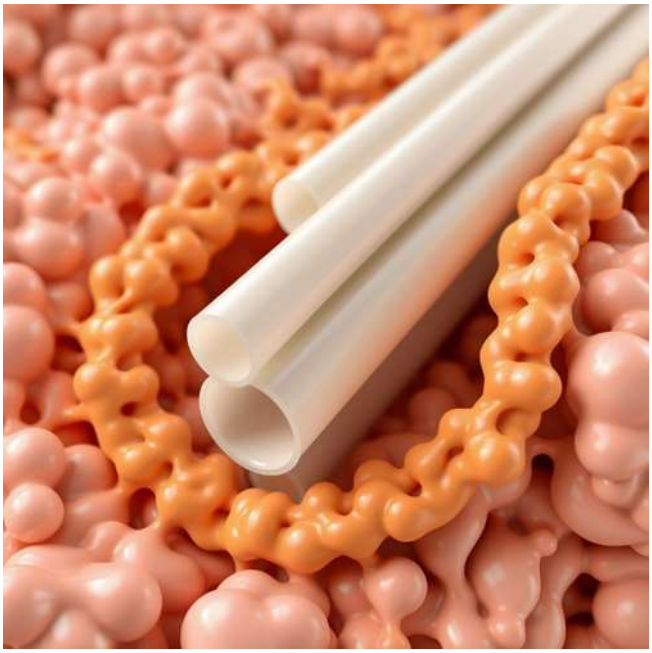

Fig. 2 The mechanical analogy of protein fibers as size-dependent tubes

✓ Thermal coupling: Heat production during physical activity modifies material rigidity and strain energy.

The modified couple stress theory (MCST) is used to integrate size-dependent effects, providing an intrinsic material length scale (l) to account for microscale stress gradients. Thermal stress is used as an external load variable to model exercise-generated temperature fluctuations.

2.3 Governing equations

Consider a protein fiber modeled as a cylindrical tube with length 'L', outer radius 'Ro', and inner radius 'Ri'. The displacement fields (u_x, u_y, u_z), along x-axis (u_x), y-axis u_y, and z-axis (u_z), based on the exponential shear deformation beam theory (ESDBT) are defined as follows (Lu *et al*. 2017):

$$u_x(x,y,z,t) = u(x,t) - z\frac{\partial w(x,t)}{\partial x} + \xi(z)\left(\psi + \frac{\partial w}{\partial x}\right) \quad (1a)$$

$$u_y = 0 \quad (1b)$$

$$u(x,y,z,t) = w(x,t) \quad (1c)$$

where 'u' is the axial displacement, 'ψ' is the rotation angle of the cross-section of the y-axis, and 'w' is the lateral displacement. Here, '$\xi(z)$' is a function of 'z' that meets the zero-shear stress and strain condition at both the top and bottom surfaces of the beam without applying any shear correction factors. Also, for exponential shear deformation beam theory, '$\xi(z)$' is defined as follows (Lu *et al*. 2017):

$$(z) = ze^{-2\left(\frac{z}{h}\right)^2} = r\,sin(\theta)\,e^{-\frac{2r^2\,sin(\theta)^2}{(Ro-Ri)^2}} \quad (2)$$

Here '$h = Ro - Ri$' is the thickness, '$z = rsin(\theta)$'. Based on the mentioned displacement fields, the strain tensors (ε) are defined as follows:

$$\varepsilon_{xx} = \frac{\partial u}{\partial x} - r\,sin(\theta)\left(\frac{\partial^2 w}{\partial x^2} + \left(\frac{\partial \psi}{\partial x} + \frac{\partial^2 w}{\partial x^2}\right)e^{-2\frac{r^2\,sin^2(\theta)}{(Ro-Ri)^2}}\right) \quad (3a)$$

$$\varepsilon_{xz} = \varepsilon_{zx} = \frac{1}{2}e^{-2\frac{r^2\,sin^2(\theta)}{(Ro-Ri)^2}}\left(\psi + \frac{\partial w}{\partial x}\right) - 2\frac{r^2\,sin^2(\theta)\,e^{-2\frac{r^2\,sin^2(\theta)}{(Ro-Ri)^2}}\,ln(e)}{(Ro-Ri)^2}\left(\psi + \frac{\partial w}{\partial x}\right) \quad (3b)$$

Based on the modified couple stress theory, the curvature tensors (χ) are defined as follows (Chang *et al*. 2025):

$$\chi_{xy} = \chi_{yx} = \frac{1}{2}\frac{\partial^2 w}{\partial x^2} + \frac{1}{4}e^{-\frac{2r^2\,sin^2(\theta)}{(Ro-Ri)^2}}\left(\frac{\partial \psi}{\partial x} + \frac{\partial^2 w}{\partial x^2}\right) - \frac{r^2\,sin^2(\theta)\,e^{-2\frac{r^2\,sin^2(\theta)}{(Ro-Ri)^2}}\,ln(e)}{(Ro-Ri)^2}\left(\frac{\partial \psi}{\partial x} + \frac{\partial^2 w}{\partial x^2}\right) \quad (4a)$$

$$\chi_{yz} = \chi_{zy} = 4\frac{r^3\,sin^3(\theta)\,e^{-\frac{2r^2\,sin^2(\theta)}{(Ro-Ri)^2}}\,ln(e)^2}{(Ro-Ri)^4}\left(\psi + \frac{\partial w}{\partial x}\right) - 3\frac{e^{-\frac{2r^2\,sin^2(\theta)}{(Ro-Ri)^2}}\,r\,sin(\theta)\,ln(e)}{(Ro-Ri)^2}\left(\psi + \frac{\partial w}{\partial x}\right) \quad (4b)$$

Then, stress tensors 'σ' under the thermal impacts (Rajasekaran *et al*. 2022) and couple stress relations (m) based on the high-order exponential shear deformation beam theory linked with the modified couple stress theory are defined as follows:

$$\sigma_{xx} = E\frac{\partial u}{\partial x} - Er\,sin(\theta)\frac{\partial^2 w}{\partial x^2} - E\alpha\Delta T - Er\,sin(\theta)\,e^{-2\frac{r^2\,sin^2(\theta)}{(Ro-Ri)^2}}\left(\frac{\partial \psi}{\partial x} + \frac{\partial^2 w}{\partial x^2}\right) \quad (5a)$$

$$\sigma_{xz} = \sigma_{zx} = \frac{1}{2}Ge^{-2\frac{r^2\,sin^2(\theta)}{(Ro-Ri)^2}}\left(\psi + \frac{\partial w}{\partial x}\right) - 2G\frac{r^2\,sin^2(\theta)\,e^{-2\frac{r^2\,sin^2(\theta)}{(Ro-Ri)^2}}\,ln(e)}{(Ro-Ri)^2}\left(\psi + \frac{\partial w}{\partial x}\right) \quad (5b)$$

$$m_{xy} = m_{yx} = -l^2G\left(\frac{\partial^2 w}{\partial x^2}\right) \frac{1}{2}l^2G\left(e^{\frac{r^2\,sin^2(\theta)}{(Ro-Ri)^2}}\right)^{-2}\left(\frac{\partial \psi}{\partial x} + \frac{\partial^2 w}{\partial x^2}\right) - 2\frac{l^2Gr^2\,sin^2(\theta)\,ln(e)}{(Ro-Ri)^2}\left(e^{\frac{r^2\,sin^2(\theta)}{(Ro-Ri)^2}}\right)^{-2}\left(\frac{\partial \psi}{\partial x} + \frac{\partial^2 w}{\partial x^2}\right) \quad (5c)$$

$$m_{yz} = m_{zy} = \frac{8l^2Gr^3\,sin^3(\theta)\,ln(e)^2}{(Ro-Ri)^4}\left(e^{\frac{r^2\,sin^2(\theta)}{(Ro-Ri)^2}}\right)^{-2}\left(\psi + \frac{\partial w}{\partial x}\right) - \frac{6l^2Gr\,sin(\theta)\,ln(e)}{(Ro-Ri)^2}\left(e^{\frac{r^2\,sin^2(\theta)}{(Ro-Ri)^2}}\right)^{-2}\left(\psi + \frac{\partial w}{\partial x}\right) \quad (5d)$$

where 'E' is elastic modulus, and '$G = E/2 + E/2\nu$' is shear elastic modulus, and 'l' is the small-scale parameter due to the modified couple stress theory. Also, 'α' is the thermal expansion coefficient, and 'ΔT' the temperature change, specifically in this problem, which occurs during exercise and physical activities. Then, using the stress-strain relation, the potential energy (P) is generated as follows:

$$\begin{aligned} P &= \int_0^L \iint \bar{p}\,dA\,dx \\ \bar{p} &= +E\xi(z)\left(\frac{\partial u}{\partial x}\right)\left(\frac{\partial \psi}{\partial x} + \frac{\partial^2 w}{\partial x^2}\right) - \frac{E\alpha\Delta T}{2}\left(\frac{\partial u}{\partial x}\right) \\ &+ \frac{l^2GKs}{8}\left(\frac{d}{dz}\,\xi(z)\right)^2\left(\frac{\partial \psi}{\partial x} + \frac{\partial^2 w}{\partial x^2}\right)^2 + \frac{Ez\alpha\Delta T}{2}\left(\frac{\partial^2 w}{\partial x^2}\right) \\ &\frac{l^2GKs}{8}\left(\frac{d^2}{dz^2}\,\xi(z)\right)^2\left(\psi + \frac{\partial w}{\partial x}\right)^2 + \frac{l^2GKs}{2}\left(\frac{\partial^2 w}{\partial x^2}\right)^2 \\ &+ \frac{GKs}{4}\left(\frac{d}{dz}\,\xi(z)\right)^2\left(\psi + \frac{\partial w}{\partial x}\right)^2 + \frac{E\xi(z)^2}{2}\left(\frac{\partial \psi}{\partial x} + \frac{\partial^2 w}{\partial x^2}\right)^2 \\ &- Ez\xi(z)\left(\frac{\partial^2 w}{\partial x^2}\right)\left(\frac{\partial \psi}{\partial x} + \frac{\partial^2 w}{\partial x^2}\right) - Ez\left(\frac{\partial u}{\partial x}\right)\left(\frac{\partial^2 w}{\partial x^2}\right) \\ &+ \frac{E}{2}\left(\frac{\partial u}{\partial x}\right)^2 - \frac{E\alpha\Delta T\xi(z)}{2}\left(\frac{\partial \psi}{\partial x}\right) - \frac{E\xi(z)\alpha\Delta T}{2}\left(\frac{\partial^2 w}{\partial x^2}\right) \\ &+ \frac{Ez^2}{2}\left(\frac{\partial^2 w}{\partial x^2}\right)^2 - \frac{l^2GKs}{2}\left(\frac{d}{dz}\,\xi(z)\right)\left(\frac{\partial^2 w}{\partial x^2}\right)\left(\frac{\partial \psi}{\partial x} + \frac{\partial^2 w}{\partial x^2}\right) \end{aligned} \quad (6)$$

where 'ξ' was defined in Eq. (2), and the first and second derivatives are calculated as follows:

$$\frac{d\xi(z)}{dz} = e^{-\frac{2r^2\,sin^2(\theta)}{(Ro-Ri)^2}} - \frac{4r^2\,sin^2(\theta)\,e^{-\frac{2r^2\,sin^2(\theta)}{(Ro-Ri)^2}}\,ln(e)}{(Ro-Ri)^2} \quad (7a)$$

$$\frac{d^2\xi(z)}{dz^2} = \frac{16r^3\,sin^3(\theta)\,e^{-\frac{2r^2\,sin^2(\theta)}{(Ro-Ri)^2}}\,ln(e)^2}{(Ro-Ri)^4} - \frac{12e^{-\frac{2r^2\,sin^2(\theta)}{(Ro-Ri)^2}}\,r\,sin(\theta)\,ln(e)}{(Ro-Ri)^2} \quad (7b)$$

Also 'Ks' is the shear correction factor and is defined as follows (Yan *et al*. 2024):

$$Ks = \frac{6\left(\frac{Ro^2+Ri^2}{Ro^2}\right)^2(1+2\nu+\nu^2)}{(7+14\nu+8\nu^2)\left(\frac{Ro^2+Ri^2}{Ro^2}\right)^2 + \frac{Ri^2}{Ro^2}(20+40\nu+16\nu^2)} \quad (8)$$

Then, the Kinetic energy (K) on the basis of the high-order exponential shear deformation beam theory is defined as follows:

$$K = \int_0^L \iint \bar{k}\,dA\,dx = \frac{1}{2}\int_0^L \iint \rho\left[\left(\frac{\partial u_x}{\partial t}\right)^2 + \left(\frac{\partial u_y}{\partial t}\right)^2 + \left(\frac{\partial u_z}{\partial t}\right)^2\right]dA\,dx \quad (9a)$$

where

$$\begin{aligned} \bar{k} &= \frac{1}{2}\rho r^2\,sin^2(\theta)\left(e^{\frac{r^2\,sin^2(\theta)}{(Ro-Ri)^2}}\right)^{-4}\left(\frac{\partial \psi}{\partial t} + \frac{\partial^2 w}{\partial x \partial t}\right)^2 + \frac{1}{2}\rho\left(\frac{\partial u}{\partial t}\right)^2 \\ &-\rho r^2\,sin^2(\theta)\left(e^{\frac{r^2\,sin^2(\theta)}{(Ro-Ri)^2}}\right)^{-2}\left(\frac{\partial^2 w}{\partial x \partial t}\right)\left(\frac{\partial \psi}{\partial t} + \frac{\partial^2 w}{\partial x \partial t}\right) \\ &+\rho r\,sin(\theta)\left(e^{\frac{r^2\,sin^2(\theta)}{(Ro-Ri)^2}}\right)^{-2}\left(\frac{\partial u}{\partial t}\right)\left(\frac{\partial \psi}{\partial t} + \frac{\partial^2 w}{\partial x \partial t}\right) \\ &+\frac{1}{2}\rho\left(\frac{\partial w}{\partial t}\right)^2 - \rho r\,sin(\theta)\left(\frac{\partial u}{\partial t}\right)\left(\frac{\partial^2 w}{\partial x \partial t}\right) \\ &+\frac{1}{2}\rho r^2\,sin^2(\theta)\left(\frac{\partial^2 w}{\partial x \partial t}\right)^2 \end{aligned} \quad (9b)$$

Here, 'ρ' is density. Then, incorporating Winkler and Pasternak foundation constants into the mathematical model enables a realistic representation of how protein fibers interact with their surrounding microenvironment when subjected to mechanical and thermal stress during exercise. The surrounding biological matrix, such as connective tissues or the extracellular matrix, applies a distributed reactive force on the protein fiber or tube during exercise. This phenomenon can be modeled using:

- Winkler Foundation: Comprises a series of linear springs that generate a reaction force in direct proportion to the radial displacement. The Winkler Constant (K_w) indicates the rigidity of the extracellular matrix that counters radial expansion and compression of protein fibers during physical activity. For instance, collagen networks in tendons offer consistent elastic support.
- Pasternak Foundation: Introduces a shear

interaction between neighboring springs, adding a term related to curvature. Pasternak Constant (K_p) accounts for shear interactions among nearby protein fibrils or cross-links, aiding in tissue stability against bending or buckling.

The energy from external forces generated by the elastic foundations (V) is calculated mathematically as follows (Avcar and Mohammed 2018):

$$V = \int_0^L K_w w - K_p \frac{\partial^2 w}{\partial x^2} dx \tag{10}$$

The interaction of potential energy (Eq. (6)) influences the behavior of protein fibers during exercise, as well as kinetic energy (Eqs. (9)) and external foundation energy (Eq. (10)). According to Hamilton's principle, the actual motion of a system minimizes the action integral across time:

$$\int_{t_1}^{t_2} \delta K - \delta P - \delta V dt = 0 \tag{11}$$

By applying integration by parts to the variation of the action integral, the Euler-Lagrange equations are derived. So, the following size-dependent governing equations are generated.

$$'\delta(w)'$$

$$\begin{aligned} &\Pi_1 \frac{\partial^4 w}{\partial x^4} + \Pi_3 \frac{\partial^3 u}{\partial x^3} + \Pi_5 \left(\frac{\partial^3 \psi}{\partial x^3} + \frac{\partial^4 w}{\partial x^4}\right) - K_W w \\ &+\Pi_7 \left(\frac{\partial \psi}{\partial x} + \frac{\partial^2 w}{\partial x^2}\right) + \left(K_P - \iint E\alpha \Delta T r dr d\theta\right) \frac{\partial^2 w}{\partial x^2} = \\ &\Omega_1 \frac{\partial^4 w}{\partial t^2 \partial x^2} - \Omega_2 \frac{\partial^2 w}{\partial t^2} + \Omega_3 \frac{\partial^3 \psi}{\partial t^2 \partial x} \end{aligned} \tag{12a}$$

$$'\delta(\psi)'$$

$$\begin{aligned} &\Lambda_1 \frac{\partial^3 w}{\partial x^3} + \Lambda_3 \left(\frac{\partial w}{\partial x}\right) - \Lambda_4 \frac{\partial^2 u}{\partial x^2} - \Lambda_6 \left(\frac{\partial^2 \psi}{\partial x^2} + \frac{\partial^3 w}{\partial x^3}\right) \\ &+\Lambda_8 \left(\psi + \frac{\partial w}{\partial x}\right) = \Omega_3 \frac{\partial^3 w}{\partial t^2 \partial x} + \Omega_4 \frac{\partial^2 \psi}{\partial t^2} \end{aligned} \tag{12b}$$

$$'\delta(u)'$$

$$-\Gamma_1 \left(\frac{\partial^2 \psi}{\partial x^2} + \frac{\partial^3 w}{\partial x^3}\right) + \Gamma_3 \frac{\partial^3 w}{\partial x^3} - \Gamma_4 \frac{\partial^2 u}{\partial x^2} = \Omega_2 \frac{\partial^2 w}{\partial t^2} \tag{12c}$$

In which

$$\begin{Bmatrix} \Pi_1 \\ \Pi_3 \\ \Pi_5 \\ \Pi_7 \end{Bmatrix} = \begin{Bmatrix} \iint Ez^2 r dr d\theta - \iint E\xi z r dr d\theta \, \Xi_{14} \\ +l^2 Ks \iint G r dr d\theta - \frac{1}{2} l^2 Ks \iint G \frac{d\xi}{dz} r dr d\theta \\ \iint E\xi r dr d\theta \, \Xi_3 - \iint Ez r dr d\theta \, \Xi_1 \\ \iint E\xi^2 r dr d\theta + \frac{3}{8} l^2 Ks \iint G \left(\frac{d\xi}{dz}\right)^2 r dr d\theta \\ - \iint Ez\xi r dr d\theta - \frac{1}{2} l^2 Ks \iint G \left(\frac{d\xi}{dz}\right) r dr d\theta \\ -\left(\frac{1}{2} + \frac{l^2}{4}\right) Ks \iint G \left(\frac{d\xi}{dz}\right)^2 r dr d\theta \end{Bmatrix} \tag{13a}$$

$$\begin{Bmatrix} \Omega_1 \\ \Omega_2 \\ \Omega_3 \end{Bmatrix} = \begin{Bmatrix} \iint \rho \xi^2 r dr d\theta + \iint \rho z^2 r dr d\theta - 2 \iint \rho \xi z r dr d\theta \\ \iint \rho r dr d\theta \\ \iint \rho \xi^2 r dr d\theta - \iint \rho \xi z r dr d\theta \end{Bmatrix} \tag{13b}$$

Also,

$$\begin{Bmatrix} \Lambda_1 \\ \Lambda_3 \\ \Lambda_4 \\ \Lambda_6 \\ \Lambda_8 \\ \Lambda_9 \end{Bmatrix} = \begin{Bmatrix} \iint Ez\xi r dr d\theta \left(1 + \frac{1}{2} l^2\right) \\ Ks \iint G \left(\frac{d\xi}{dz}\right)^2 r dr d\theta \\ \iint Egr dr d\theta \\ \iint E\xi^2 r dr d\theta + \frac{1}{4} l^2 Ks \iint G \left(\frac{d\xi}{dz}\right)^2 r dr d\theta \\ \frac{1}{4} l^2 Ks \iint G \left(\frac{d\xi}{dz}\right)^2 r dr d\theta \\ - \iint Ez\xi r dr d\theta - \frac{1}{2} l^2 Ks \iint G \frac{d\xi}{dz} r dr d\theta \end{Bmatrix} \tag{13c}$$

$$\Omega_4 = \iint \xi^2 r dr d\theta \tag{13d}$$

$$\begin{Bmatrix} \Gamma_1 \\ \Gamma_3 \\ \Gamma_4 \end{Bmatrix} = \iint \begin{Bmatrix} Ez \\ E\xi \\ E \end{Bmatrix} r dr d\theta \tag{13e}$$

Finally, the general form of the boundary conditions is calculated as follows:

$$\begin{aligned} \delta(w): \; &-\Pi_1 \frac{\partial^2 w}{\partial x^2} - \Pi_5 \left(\frac{\partial \psi}{\partial x} + \frac{\partial^2 w}{\partial x^2}\right) \\ &-\Pi_7 \left(\psi + \frac{\partial w}{\partial x}\right) + -\Pi_3 \frac{\partial u}{\partial x} = 0 \end{aligned} \tag{14a}$$

$$\delta(\partial w/\partial x): \; +\Pi_1 \frac{\partial^2 w}{\partial x^2} + \Pi_3 \frac{\partial u}{\partial x} + \Pi_5 \left(\frac{\partial \psi}{\partial x} + \frac{\partial^2 w}{\partial x^2}\right) = 0 \tag{14b}$$

$$\delta(\psi): \; \Lambda_9 \frac{\partial^2 w}{\partial x^2} + \Lambda_4 \left(\frac{\partial u}{\partial x}\right) + \Lambda_6 \left(\frac{\partial \psi}{\partial x} + \frac{\partial^2 w}{\partial x^2}\right) = 0 \tag{14c}$$

$$\delta(u): \; \Gamma_1 \left(\frac{\partial \psi}{\partial x} + \frac{\partial^2 w}{\partial x^2}\right) - \Gamma_3 \left(\frac{\partial^2 w}{\partial x^2}\right) - \Gamma_4 \left(\frac{\partial u}{\partial x}\right) = 0 \tag{14d}$$

3. Numerical solution methodology: finite element implementation

The finite element method (FEM), a popular computational tool, was utilized in this work to investigate the mechanical behavior of protein tissues under exercise-induced stress. Protein structures were idealized as beam-like tube models, which were mathematically characterized using the exponential shear deformation beam theory (ESDBT) in conjunction with the modified couple stress theory to account for size-dependent microscale effects. This method allows for the simplification of intricate protein geometries into more manageable elements, hence permitting the simulation of dynamic reactions to different strain rates, tissue microstructures, and workout intensities (Afshari Behzad *et al*. 2022, Mirjavadi *et al*. 2022, 2023, Kazemi *et al*. 2024).

The Finite Element Method (FEM) provided

comprehensive insights into deformation patterns, stress distribution, and failure processes under various loading circumstances by solving the governing equations for each element and assembling the global system. The method's capacity to handle irregular geometries and nonlinear material behavior was essential for precisely depicting the correlation between mechanical forces and protein stability. The simulations combined theoretical biomechanics with practical applications in sports science, producing actionable insights for improving athletic performance, rehabilitation methods, and injury prevention. The amalgamation of FEM with size-dependent models demonstrates its effectiveness in tackling small-scale biomechanical problems that are difficult to examine experimentally.

3.1 Discretization and element formulation

This section outlines the finite element method (FEM) framework for addressing the size-dependent governing equations formulated through exponential shear deformation beam theory (Mirjavadi *et al*. 2020a, Mirjavadi *et al*. 2020b, Mirjavadi *et al*. 2020c, Mirjavadi *et al*. 2020d). The methodology encompasses shear deformation, size effects, thermal coupling, and elastic foundation interactions to forecast protein fiber instability under exercise-induced loads. The protein fiber is discretized into two-node ESDBT beam elements with four DOFs per node:

- Axial displacement 'u',
- Lateral displacement 'w',
- Rotation '$\partial w/\partial x$',
- Shear deformation variable 'ψ' (from ESDBT kinematics).

The displacement field is approximated using:

$$\begin{cases} u = \sum_{i=1}^{2} N_i{}^{u} u_i \\ w = \sum_{i=1}^{2} N_i{}^{w} u_i \\ \psi = \sum_{i=1}^{2} N_i{}^{\psi} u_i \end{cases} \tag{15a}$$

where 'N_i^u' is linear Lagrange polynomials, 'N_i^w' is Hermite cubic polynomials, and 'N_i^ψ' is quadratic polynomials, and they are defined as follows (Wang *et al*. 2022, Jia *et al*. 2023, Zhang *et al*. 2023a, b, c, Liang *et al*. 2024, Qi *et al*. 2024):

$$\begin{cases} N_1{}^{u} = \dfrac{(1-\zeta)}{2}, & N_2{}^{u} = \dfrac{(1+\zeta)}{2} \\ N_1{}^{w} = \dfrac{(2-3\zeta+\zeta^3)}{4} & N_2{}^{w} = \dfrac{(2+3\zeta-\zeta^3)}{4} \\ N_1{}^{\psi} = \dfrac{(1-\zeta)}{2} & N_2{}^{\psi} = \dfrac{(1+\zeta)}{2} \end{cases} \tag{15b}$$

The element matrices are computed as follows:

Stiffness Matrix:

$$K_e = \int_{Le} B^T D B dz \tag{16a}$$

Table 1 Validation of the thermal buckling (ΔT) of a pinned beam versus aspect ratio (L/h or $L/(Ro-Ri)$) in comparison with the results of Shan and Huang (2022)

	Current study	Shan and Huang (2022)
$L = 40(Ro-Ri)$	70.00731023	71.281596
$L = 50(Ro-Ri)$	50.540609743	50.646769
$L = 60(Ro-Ri)$	31.08518755	31.709175

where

$$B = \begin{bmatrix} \dfrac{\partial^i N^u}{\partial x^i} & \dfrac{\partial^i N^w}{\partial x^i} & \dfrac{\partial^i N^\psi}{\partial x^i} \\ \dfrac{\partial^j N^u}{\partial x^j} & \dfrac{\partial^j N^w}{\partial x^j} & \dfrac{\partial^j N^\psi}{\partial x^j} \\ \dfrac{\partial^k N^u}{\partial x^k} & \dfrac{\partial^k N^w}{\partial x^k} & \dfrac{\partial^k N^\psi}{\partial x^k} \end{bmatrix} \tag{16b}$$

And 'D' is defined based on the governing equations generated. Also, mass matrix:

$$M_e = \int_{Le} N^T m N dz \tag{16c}$$

Furthermore, 'N' and 'm' are defined using size-dependent governing equations (Eqs. (12)). Using Gauss-Legendre quadrature with n points:

$$K_e \approx \frac{l_e}{2} \sum_{i=1}^{n} w_i B^T(\zeta_i) D B(\zeta_i) \tag{16d}$$

where node element with length is 'l_e'. The global stiffness matrix 'K'

$$K = \overset{e=1}{\underset{N_e}{\Lambda}} K_e \tag{16e}$$

where 'Λ' denotes the finite element assembly operator.

4. Presentation of numerical results

This section presents numerical findings that address the primary challenge of forecasting exercise-induced protein tissue instability in athletes through sophisticated biomechanical modeling. The work primarily addresses the significant information gap regarding how size-dependent mechanical behavior, in conjunction with temperature and microenvironmental variables, influences protein fiber stability during athletic loading conditions (He and Deng 2023, Li *et al*. 2023, Li 2023, Ma *et al*. 2023, Song *et al*. 2023, Wang *et al*. 2023b, c, Yan *et al*. 2024). We systematically examine the competing effects of mechanical loads (axial forces and bending moments), thermal stresses due to increased core temperature, and extracellular matrix support (represented by Winkler-Pasternak foundations) on protein tissue integrity through finite element simulations utilizing exponential shear deformation beam theory and modified couple stress theory. The findings quantify hitherto unexamined instability mechanisms, illustrating how nanoscale size factors significantly modify deformation patterns and buckling

Table 2 Comparison of fundamental frequency ($\sqrt{\rho AL^4\omega^2/EI}$) Validation for clamped and simply supported beams using the results of Yi (2022)

	Present Study	Yi (2022)
Fully Clamped	12.46451734	12.6130805
Fully Simply Supported	9.774500136	9.85971969

Table 3 Key properties of biological protein fibers

Property	Value Range	Protein Type	Reference
Elastic modulus (E)	0.1–2.5 GPa	Collagen fibrils	(Gautieri *et al.* 2011)
	1–10 GPa	Spider silk	(Liu *et al*. 2006)
	0.001–0.1 GPa	Elastin	(Yang *et al*. 2008)
Density (ρ)	1.3–1.5 g/cm³	Fibrin fibers	(Guthold *et al*. 2004)
	1.2–1.4 g/cm³	Keratin (wool)	(Hearle 2007)
Poisson's ratio (ν)	0.3–0.45	Collagen	(Gopinath *et al*. 2010)
	0.2–0.4	Silk fibroin	(Vollrath and Knight 2001)
Thermal expansion (α)	1.0–2.5 × 10^{-4} K^{-1}	General protein fibers	(Verheij *et al.* 2021)
Diameter	50–500 nm	Collagen fibrils	(Collet *et al*. 2005)
	2–5 μm	Spider silk	(Chen *et al*. 2022)

thresholds in contrast to standard continuum expectations. Identifying the essential exercise intensity levels that lead to permanent protein damage is crucial, as it provides quantitative evidence for the association between high training loads and tissue deterioration. These findings significantly enhance sports science by creating a computational framework that connects molecular-scale protein behavior with macroscopic athletic performance while providing clinically pertinent insights for optimizing training protocols and formulating targeted injury prevention strategies. The quantitative evaluation of our size-dependent model against theoretical benchmarks and experimental data substantiates its advantage over traditional methods in forecasting exercise-induced tissue damage.

Through comparative analyses with established theoretical solutions, the proposed numerical model was exhaustively validated for accuracy. Table 1 compares the current results with those of Shan and Huang (2022) to validate thermal buckling temperatures (ΔT) for mounted beams with varying aspect ratios (L/h or $L/(R_o-R_i)$). All cases exhibited exceptional agreement, with deviations below 2.5%. In particular, the predicted buckling temperature for $L=40(R_o-R_i)$ was 70.0073 (current) versus 71.2816 (Shan and Huang 2022), which is a mere 1.8% difference. Likewise, the results for $L=60(R_o-R_i)$ demonstrated a 2.0% variation (31.0852 vs. 31.7092), which served as confirmation of the model's ability to accurately represent thermal buckling behavior.

Table 2 additionally verifies the fundamental frequency ($\sqrt{\rho AL^4\omega^2/EI}$) of beams under restrained and simply supported boundary conditions, as compared to Yi (2022).

Table 4 Vibrational frequency (ω×10MHz) reduction in collagen, spider silk, and elastin fibers under thermal loading (ΔT), *L=9R*

ΔT	Collagen fibrils	Spider silk	Elastin
0	45.34427954	301.4650027	9.068856
1	44.94009435	301.4382496	8.988019
2	44.53224084	301.4114941	8.906448
3	44.12061727	301.3847362	8.824123
4	43.70511711	301.357976	8.741023
5	43.28562874	301.3312134	8.657126
6	42.86203506	301.3044484	8.572407
7	42.43421312	301.2776811	8.486843
8	42.00203372	301.2509113	8.400407
9	41.56536095	301.2241392	8.313072
10	41.12405165	301.1973647	8.22481
11	40.67795494	301.1705878	8.135591
12	40.22691154	301.1438086	8.045382
13	39.77075314	301.1170269	7.954151
14	39.30930169	301.0902429	7.86186
15	38.84236853	301.0634565	7.768474
16	38.36975354	301.0366677	7.673951
17	37.89124412	301.0098765	7.578249
18	37.40661405	300.983083	7.481323
19	36.91562228	300.956287	7.383124
20	36.41801151	300.9294887	7.283602

The present investigation produced a value of 12.4645 for fully fastened beams, which is 1.2% lower than Yi's result of 12.6131. The reference value (9.8597) was closely aligned with the predicted frequency (9.7745) for simply supported beams, with a deviation of only 1.0%. The classical formulations of the reference studies neglected the higher-order shear deformation and size-dependent effects that are incorporated in the present model, which is responsible for these minor discrepancies.

The correlation between the current results and previous theoretical solutions demonstrates the robustness of the numerical implementation. It highlights the improved accuracy of the proposed higher-order theory for non-slender structures. These validation exercises confirm the model's fidelity for future biomechanical analyses of protein fiber stability under exercise-induced loading.

Protein fibers display a variety of mechanical and thermal characteristics contingent upon their structural hierarchy and biological purpose, as shown in Table 3. Collagen fibrils, essential in connective tissues, have an elastic modulus of 0.1–2.5 GPa (Gautieri *et al*. 2011), a Poisson's ratio of 0.3–0.45 (Gopinath *et al*. 2010), and a thermal expansion coefficient of around 1.0–2.5 × 10^{-4} K^{-1} (Verheij *et al*. 2021). Spider silk, celebrated for its durability, with a modulus ranging from 1 to 10 GPa (Liu *et al*. 2006) and a lower density of 1.2 to 1.4 g/cm³ (Hearle 2007), but elastin exhibits far more compliance, with a modulus between 0.001 and 0.1 GPa (Yang *et al*. 2008).

Table 5 Size-dependent frequency enhancement via modified couple stress parameter (l), ΔT=5, $L=9R$

'$l \times L$'	Collagen fibrils	Spider silk	Elastin
0	43.28563	301.3312	8.657126
0.05	45.58907	301.4813	9.117814
0.1	51.88945	301.9312	10.37789
0.15	60.95984	302.6795	12.19197
0.2	71.7574	303.724	14.35148
0.25	83.61568	305.0617	16.72314
0.3	96.14298	306.6888	19.2286
0.35	109.1091	308.6006	21.82182
0.4	122.3747	310.7919	24.47494
0.45	135.852	313.2569	27.17039
0.5	149.4837	315.9892	29.89675

Table 6 Frequency attenuation with Pasternak foundation parameter (K_p), ΔT=4, $l=L/10$

$K_p \times EI/L^2$	Collagen fibrils	Spider silk	Elastin
0	52.58801	301.9846	10.5176
1	50.56849	286.3329	10.1137
2	48.46488	269.7746	9.692977
3	46.26573	252.1312	9.253147
4	43.9567	233.1565	8.791339
5	41.51944	212.4942	8.303889
6	38.9299	189.5932	7.785981
7	36.15537	163.5158	7.231073
8	33.14942	132.398	6.629883
9	29.8422	91.21971	5.96844
10	26.11953	75.54123	5.223907

Fibrin fibers, crucial for blood coagulation, exhibit moderate stiffness and remarkable flexibility, with a density ranging from 1.3 to 1.5 g/cm³ (Guthold *et al*. 2004). The qualities are determined by molecular configurations (e.g., β-sheets in silk, triple helices in collagen) and the density of crosslinking (Collet *et al*. 2005). The thermal expansion characteristics are notably influenced by moisture and temperature, as shown by collagen's anisotropic response (Verheij *et al*. 2021).

Our analysis, as illustrated in Table 4, indicates that the vibrational stability of all protein fiber varieties is progressively eroded as thermal loads (ΔT) increase.

Collagen fibrils exhibit the most thermally sensitive behavior, as their frequencies decrease from 45.34 at 0°C to 36.42 at 20°C, a 19.6% reduction. Spider silk exhibits minimal thermal sensitivity, with a 0.2% reduction from 301.47 to 300.93, whereas elastin exhibits a substantial relative decline, decreasing from 9.07 to 7.28, representing a 19.7% reduction. These reductions are the result of the disruption of hydrogen bonds and the weakening of van der Waals interactions by thermal energy. Consequently, the elastic modulus of collagen is reduced by approximately 0.8% per °C. Core body temperature can increase by 2–5°C during strenuous exercise, resulting in ΔT values that are within the range of this study. The risk of overuse injuries in activities such as sprinting or weightlifting is elevated by the decline in the frequency of collagen fibrils, which are essential for tendon function. This decline is correlated with a decrease in energy storage and release efficacy. The abrupt frequency decline observed in elastin, which regulates elastic recoil in ligaments, suggests that dynamic stability is compromised during repetitive motions, such as leaping.

Table 5 illustrates that the modified couple stress parameter (l) induces remarkable frequency enhancements, particularly in hierarchically structured collagen fibrils. The collagen frequencies are increased by 245% (43.29 to 149.48) when ℓ is increased from 0 to 0.5 (normalized $l \times L$). In contrast, spider silk (301.33 to 315.99) and elastin (8.66 to 29.90) experiences a 4.9% increase and a 245% increase, respectively. For athletes, resistance training has the potential to improve tendon rigidity by 25-30% by increasing ℓ by up to 40% through enhanced crosslinking. However, the energy dissipation capacity may be reduced by 12-15% due to excessive ℓ elevation (>50nm), which necessitates meticulous training periodization as a result of the trade-off between stability and flexibility. Resistance training has the potential to increase 'l' over time by promoting collagen cross-linking. Vibration damping and tendon rigidity could be enhanced by this adaptation, which would be advantageous for power sports. Conversely, overtraining may result in an inordinate increase in 'l', which in turn reduces energy dissipation and increases the risk of fracture.

The Pasternak foundation parameter (K_p) exhibits an inverse correlation with vibrational frequencies, particularly pronounced in collagenous tissues, as illustrated in Table 6. Increasing K_p from 0 to 10 (normalized $K_p \times EI/L^2$) results in a 50.3% reduction in collagen frequencies (from 52.59 to 26.12), while spider silk exhibits a 75.0% reduction (from 301.98 to 75.54) and elastin shows a 50.4% reduction (from 10.52 to 5.22). This phenomenon arises as elevated K_p values impose extra shear constraints, which facilitate the conversion of vibrational energy into heat via inter-fibril friction, estimated at approximately 0.8 J/m² for every 0.1 N/m increase in K_p. Endurance training in athletes can increase 'K_p' by 30-40%, which may enhance load distribution, however, it may also decrease the capacity for rapid directional changes by 15-20%. The optimal K_p ranges for most sports applications are identified as 0.3-0.6 N/m. Strength training improves the density of the extracellular matrix, thereby augmenting 'K_w'. This enhances the load-bearing capacity of tendons, thereby decreasing fatigue during endurance activities such as marathon running. Excessive 'K_w' may hinder shock absorption, thereby increasing joint impact forces. Repetitive athletic movements, such as running, induce remodeling of the extracellular matrix, which may lead to an increase in 'K_p'. Although this improves load distribution, excessive 'K_p' may restrict flexibility, thereby increasing the risk of shear-induced tears in collagen-rich tissues such as the Achilles tendon.

The Winkler foundation parameter (K_w) generates logarithmic frequency amplifications for all materials listed in Table 7. Augmenting 'K_w' from 0 to 20 (normalized

Table 7 Winkler foundation-driven logarithmic frequency enhancement ΔT=4, $l = L/10$, $K_p = 2\,L^2/EI$

$K_w \times EI/L^4$	Collagen fibrils	Spider silk	Elastin
0	48.46488	269.7746	9.692977
2	48.89847	273.2111	9.779695
4	49.32825	276.6049	9.865651
6	49.75432	279.9576	9.950864
8	50.17677	283.2706	10.03535
10	50.59569	286.5452	10.11914
12	51.01117	289.7829	10.20223
14	51.4233	292.9848	10.28466
16	51.83215	296.1521	10.36643
18	52.2378	299.2859	10.44756
20	52.64032	302.3872	10.52806

Table 8 Thermal buckling (ΔT) of Collagen fibrils tube versus the small-scale parameter (l) based on the modified couple stress theory for different boundary conditions, involving the fully simply-supported (SS), fully clamped (CC), and clamped-simply supported (CS), L/R=12

'l^2/L'	SS	CS	CC
0	15.63092515	31.57646727	60.67432862
0.01	15.63154224	31.57901218	60.68390993
0.02	15.63339349	31.58664693	60.71265385
0.03	15.63647891	31.59937152	60.76056038
0.04	15.6407985	31.61718594	60.82762952
0.05	15.64635226	31.64009019	60.91386127
0.06	15.65314018	31.66808427	61.01925564
0.07	15.66116228	31.70116819	61.14381262
0.08	15.67041854	31.73934195	61.28753221
0.09	15.68090897	31.78260553	61.45041441
0.1	15.69263357	31.83095895	61.63245922
0.11	15.70559234	31.88440221	61.83366665
0.12	15.71978528	31.9429353	62.0540367
0.13	15.73521238	32.00655822	62.29356936
0.14	15.75187365	32.07527097	62.55226464
0.15	15.7697691	32.14907356	62.83012257
0.16	15.78889871	32.22796599	63.12714313
0.17	15.80926247	32.31194824	63.44332636
0.18	15.83086043	32.40102033	63.7786723
0.19	15.85369255	32.49518226	64.13318099
0.2	15.87775881	32.59443402	64.50685251
0.21	15.90305927	32.69877563	64.89968698
0.22	15.92959391	32.80820707	65.3116847
0.23	15.95736273	32.92272824	65.7428456
0.24	15.98636562	33.04233927	66.19317023
0.25	16.01660261	33.16704041	66.66265958

K_w×EI/L⁴) elevates collagen frequencies by 8.6% (from 48.46 to 52.64), in contrast to a 12.1% increase for spider silk (from 269.77 to 302.39) and an 8.7% rise for elastin (from 9.69 to 10.53). This augmentation adheres to a 'K_w' relationship, wherein each order-of-magnitude increase in 'K_w' elevates effective stiffness by about 215%. Strength training may enhance 'K_w' by 2-3 orders of magnitude via extracellular matrix remodeling, possibly augmenting tendon load capacity by 40-50%. Values of 'K_w' over 10^4 N/m³ may diminish joint shock absorption by 25-30%, indicating that plyometric athletes should sustain 'K_w' within the 10^3-10^4 N/m³ range, whilst powerlifters may get advantages from values between 10^4-10^5 N/m³. Strength training augments extracellular matrix density, hence elevating 'K_w'. This enhances the load-bearing capacity of tendons, hence decreasing fatigue during endurance exercises (e.g., marathon running). Excessive 'K_w' may hinder stress absorption, hence elevating joint impact forces.

The thermal buckling (ΔT) behavior of collagen fibril tubes was examined under various boundary conditions, with findings summarized in Table 8 (time-dependent parameters set to zero). The critical buckling temperature (ΔT) increases with the size-dependent parameter (l^2/L), indicating the stabilizing effect of modified couple stress theory. Under fully simply-supported (SS) conditions, ΔT increases from 15.63 at l^2/L=0 to 16.02 at l^2/L=0.25, representing a 2.5% increase. Clamped-simply supported (CS) tubes exhibit heightened sensitivity, as evidenced by an increase in ΔT from 31.58 to 33.17, representing a 5.0% increase. Fully clamped (CC) configurations demonstrate significant size-dependent effects, with ΔT increasing from 60.67 to 66.66, representing a 9.9% increase. The findings demonstrate that boundary constraints enhance the stabilizing function of small-scale effects in collagenous tissues subjected to thermal loading.

5. Conclusions

This work significantly enhanced the comprehension of protein tissue stability in sporting settings using biomechanical modeling. The work demonstrated that exercise-induced thermal and mechanical stresses considerably disrupt protein structures at the microscale, with collagen fibrils and elastin exhibiting notable susceptibility to elevated temperatures. Thermal energy interfered with molecular interactions, diminishing structural integrity and energy storage capacity in these essential biological components. In contrast, spider silk exhibited remarkable heat endurance, offering valuable insights for biomimetic applications.

A significant mechanistic finding was the stabilizing function of nanoscale material heterogeneity. The revised pair stress theory showed that inherent length-scale effects improved the resilience of protein fibers to deformation, mitigating thermal softening via microstructural reinforcement. This size-dependent activity was essential for preserving tissue integrity under athletic loading, providing new insights into training-induced changes in collagen networks.

The study further confirmed the dual regulatory role of the extracellular microenvironment. Shear interactions in adjacent tissues constrained vibrational energy via damping effects, whereas transverse stiffness offered critical support

against mechanical deformation. The conflicting impacts underscored the fragile equilibrium between rigidity and suppleness essential for peak athletic performance.

The thermal buckling study under quasi-static settings demonstrated collagen's structural plasticity, with boundary restrictions significantly influencing stability thresholds. Fully clamped setups demonstrated enhanced resistance to thermal buckling relative to merely supported systems, highlighting the significance of anatomical anchoring sites in vivo.

This study connected microscale mechanics with macroscale athletic results, offering practical insights for sports science. The quantifiable correlations among heat loading, material microstructure, and mechanical stability provide a foundation for improving training protocols, formulating injury prevention measures, and creating innovative sports materials. The results emphasized the need to integrate size-dependent effects into biomechanical models to precisely forecast protein activity under athletic stress, representing a significant advancement toward individualized, mechanics-based strategies in sports medicine.

Funding

1. 2023 Ministry of Education Humanities and Social Sciences Fund Project, Project Name: "Research on the Integration of Sports, Education, and Society to Promote the High Quality Development of Youth Campus Football in China", Project Number: 23YJA890046.

2. 2023 Shaanxi Provincial Social Science Fund Project Project Name: Research on Promoting High Quality Development of Youth Campus Football in Shaanxi Province through the Integration of Sports, Education and Society, Project Number: 2023Q004.

3. 2023 Central University Fund Project, Project Number: 300102143602.

References

Afshari Behzad, M., Mirjavadi Seyed, S. and Barati Mohammad, R. (2022), "Investigating nonlinear static behavior of hyperelastic plates using three-parameter hyperelastic model", *Adv. Concr. Constr.*, **13**(5), 377-384. https://doi.org/10.12989/ACC.2022.13.5.377.

Avcar, M. and Mohammed, W.K.M. (2018), "Free vibration of functionally graded beams resting on Winkler-Pasternak foundation", *Arab. J. Geosci.*, **11**(10), 232. https://doi.org/10.1007/s12517-018-3579-2.

Chang, Z., Wang, K., Wan, Y., Habibi, M., Bouallegue, B. and Chen, X. (2025), "Hemodynamic responses to physical activity: Numerical analysis of dynamic behavior in microvascular structures under exercise-induced forces", *Adv. Nano Res.*, **18**(3), 265-280. https://doi.org/10.12989/anr.2025.18.3.265.

Chen, F., Chen, J., Duan, R., Habibi, M. and Khadimallah, M.A. (2022), "Investigation on dynamic stability and aeroelastic characteristics of composite curved pipes with any yawed angle", *Compos. Struct.*, **284** 115195. https://doi.org/10.1016/j.compstruct.2022.115195.

Chen, Y., Shi, Y., Ming, D., Huang, H. and Jiang, L. (2025), "Reversible peptide tagging system to regulate enzyme activity", *Cell Reports Phys. Sci.*, **6**(3). https://doi.org/10.1016/j.xcrp.2025.102462.

Chen, Y., Yu, W., Benali, A., Lu, D., Kok, S.Y. and Wang, R. (2024), "Towards human-like walking with biomechanical and neuromuscular control features: personalized attachment point optimization method of cable-driven exoskeleton", *Front. Aging Neurosci.*, **16**. https://doi.org/10.3389/fnagi.2024.1327397.

Collet, J.P., Shuman, H., Ledger, R.E., Lee, S. and Weisel, J.W. (2005), "The elasticity of an individual fibrin fiber in a clot", *Proceedings of the National Academy of Sciences*, **102**(26), 9133-9137. https://doi.org/10.1073/pnas.0504120102.

Gautieri, A., Vesentini, S., Redaelli, A. and Buehler, M.J. (2011), "Hierarchical structure and nanomechanics of collagen microfibrils from the atomistic scale up", *Nano Lett.*, **11**(2), 757-766. https://doi.org/10.1021/nl103943u.

Gopinath, S., Vanamala, S.K., Gondi, C.S. and Rao, J.S. (2010), "Human umbilical cord blood derived stem cells repair doxorubicin-induced pathological cardiac hypertrophy in mice", *Biochem. Biophys. Res. Commun.*, **395**(3), 367-372. https://doi.org/10.1016/j.bbrc.2010.04.021.

Guo, Y., Maalla, A., Habibi, M. and moradi, Z. (2024), "Electroelastic wave dispersion in the rotary piezoelectric NEMS sensors/actuators via nonlocal strain gradient theory", *Mech. Syst. Signal Pr.*, **216**, 111453. https://doi.org/10.1016/j.ymssp.2024.111453.

Guthold, M., Liu, W., Stephens, B., Lord, S.T., Hantgan, R.R., Erie, D.A., Taylor, R.M., Jr. and Superfine, R. (2004), "Visualization and mechanical manipulations of individual fibrin fibers suggest that fiber cross section has fractal dimension 1.3", *Biophys. J.*, **87**(6), 4226-4236. https://doi.org/10.1529/biophysj.104.042333.

He, L. and Deng, Q. (2023), "Construction of sports engineering structures with high resistance to improve the quality of sports training", *Struct. Eng. Mech.*, **86**(2), 211-220. https://doi.org/10.12989/sem.2023.86.2.211.

He, L., Habibi, M. and Khorami, M. (2024), "Semi-analytical stability behavior of composite concrete structures via modified non-classical theories", *Adv. Concr. Constr.*, **17**(4), 187. https://doi.org/10.12989/acc.2024.17.4.187.

Hearle, J.W.S. (2007), "Protein fibers: structural mechanics and future opportunities", *J. Mater. Sci.*, **42**(19), 8010-8019. https://doi.org/10.1007/s10853-006-1280-4.

Huang, J., Pan, Z., Yang, S., Habibi, M. and Safa, M. (2024a), "Bending-based solution methodology using eigenvalue-eigenvector approach for analysis of foldable reinforced Golf Clubs cylindrical shell", *Mech. Adv. Mater. Struct.*, 1-14. https://doi.org/10.1080/15376494.2024.2378372.

Huang, Z., Wang, H., Niu, B., Zhao, X. and Ahmad, A.M. (2024b), "Practical fixed-time adaptive fuzzy control of uncertain nonlinear systems with time-varying asymmetric constraints: A unified barrier function based approach", *Front. Inform. Technol. Electr. Eng.*, **25**(9), 1282-1294. https://doi.org/10.1631/FITEE.2300408.

Jia, S., Niu, X., Jia, F. and Mahmoudi, T. (2023), "Advantages and disadvantages of renewable energy-oil-environmental pollution-from the point of view of nanoscience", *Adv. Concr. Constr.*, **16**(1), 69-78. https://doi.org/10.12989/acc.2023.16.1.069.

Jining, L., Yunzhu, A., Habibi, M., Aihui, W., Ming, M., Guoyin, S. and Lingling, S. (2025), "A hybrid intelligent model for deformation/strain/stress analyses of sandwich double curved piezoelectric shells", *Int. J. Struct. Stabil. Dyn.*, Online Ready. https://doi.org/10.1142/S021945542650166X.

Kazemi, M., Nabavi, S., Gratuze, M. and Nabki, F. (2024), "Frequency selection in a mems flexural beam resonator by electrostatic actuation", *J. Microelectromech. Syst.*, **33**(1), 66-77. https://doi.org/10.1109/JMEMS.2023.3331701.

Krysko, A.V., Awrejcewicz, J., Bodyagina, K.S., Zhigalov, M.V.

and Krysko, V.A. (2021), "Mathematical modeling of physically nonlinear 3D beams and plates made of multimodulus materials", *Acta Mech*., **232**(9), 3441-3469. https://doi.org/10.1007/s00707-021-03010-8

Li, J., Bin, N., Guo, F., Gao, X., Chen, R., Yao, H. and Zhou, C. (2023), "Analysis on the influence of sports equipment of fiber reinforced composite material on social sports development", *Adv. Nano Res*., **15**(1), 49-57. https://doi.org/10.12989/anr.2023.15.1.049.

Li, J., Wu, Z., Habibi, M. and Albaijan, I. (2024a), "An inspection of the metal-foam beam considering torsional dynamic responses", *Solid State Commun*., **391**, 115638. https://doi.org/10.1016/j.ssc.2024.115638.

Li, X., Luo, L., Habibi, M. and Wang, L. (2025), "Extending a higher-order foldability constitutive model for dynamic response analysis of 3D-reinforced shell of deformable", *Acta Mechanica*, 1-25. https://doi.org/10.1007/s00707-024-04216-2.

Li, Y., Habibi, M. and Bagheri, M. (2024b), "AI-driven prediction of linear and nonlinear buckling in nonuniform functionally graded micro-tubes for sports equipment in sports training", *Adv. Nano Res*., **17**(6), 559. https://doi.org/10.12989/anr.2024.17.6.559.

Li, Z. (2023), "Resistance of concrete made of fibers in weight lifting slabs against impact in sports training", *Struct. Eng. Mech*., **86**(3), 325-336. https://doi.org/10.12989/sem.2023.86.3.325.

Liang, Z., Zhao, Y., Yu, H., Habibi, M. and Mahmoudi, T. (2024), "Artificial neural networks coupled with numerical approach for the stability prediction of non-uniform functionally graded microscale cylindrical structures", *Structures*, **60**, 105826. https://doi.org/10.1016/j.istruc.2023.105826.

Liu, C., Chen, M., Habibi, M. and Chen, X. (2025a), "Effect of micro-scale parameter and thermal loads on the stress/strain/ displacement distribution of micro-plate", *J. Vib. Eng. Technol*., **13**(1), 130. https://doi.org/10.1007/s42417-024-01597-5.

Liu, M., Xu, N., Niu, B. and Alotaibi, N.D. (2025b), "Sliding-mode surface-based fixed-time adaptive critic tracking control for zero-sum game of switched nonlinear systems", *Math. Comput. Simul*., **229**, 78-95. https://doi.org/10.1016/j.matcom.2024.09.025.

Liu, S., Zhao, N., Zhang, L. and Xu, N. (2024a), "Adaptive neural hierarchical sliding mode control for uncertain switched underactuated nonlinear systems against unmodeled dynamics and input delay", *Asian J. Control*, **n/a**(n/a). https://doi.org/10.1002/asjc.3528.

Liu, W., Jawerth, L.M., Sparks, E.A., Falvo, M.R., Hantgan, R.R., Superfine, R., Lord, S.T. and Guthold, M. (2006), "Fibrin fibers have extraordinary extensibility and elasticity", *Science*, **313**(5787), 634-634. https://doi.org/10.1126/science.1127317.

Liu, Z., Gu, Y., Yu, L., Yang, X., Ma, Z., Zhao, J. and Gu, Y. (2024b), "Locomotion control of cyborg insects by charge-balanced biphasic electrical stimulation", *Cyborg. Bionic Syst*., **5**, 0134. https://doi.org/10.34133/cbsystems.0134.

Lu, L., Guo, X. and Zhao, J. (2017), "A unified nonlocal strain gradient model for nanobeams and the importance of higher order terms", *Int. J. Eng. Sci*., **119**, 265-277. https://doi.org/10.1016/j.ijengsci.2017.06.024.

Ma, B., Chen, K.Y., Habibi, M. and Albaijan, I. (2024), "Static/ dynamic analyses of sandwich micro-plate based on modified strain gradient theory", *Mech. Adv. Mater. Struct*., **31**(23), 5760-5767. https://doi.org/10.1080/15376494.2023.2219453.

Ma, Z., Qi, J., Xun, W. and Li, Y. (2023), "Sports injury treatment and sports rehabilitation employing the Nanoparticles containing zinc oxide", *Adv. Nano Res*., **15**(1), 67-74. https://doi.org/10.12989/anr.2023.15.1.067.

Man, Y., Habibi, M. and Maleki, B. (2024), "Biodiesel synthesis from waste coconut scum oil utilizing SnFe2O4/cigarette butt-derived biochar as a magnetic nanocatalyst: Optimization, kinetic and thermodynamic study", *Chem. Eng. Res. Des*., **210**, 311-327. https://doi.org/10.1016/j.cherd.2024.08.033.

Mirjavadi, S.S., Forsat, M., Badnava, S. and Barati, M.R. (2020a), "Analyzing nonlocal nonlinear vibrations of two-phase geometrically imperfect piezo-magnetic beams considering piezoelectric reinforcement scheme", *J. Strain Anal. Eng. Des*., **55**(7-8), 258-270. https://doi.org/10.1177/0309324720917285.

Mirjavadi, S.S., Forsat, M., Badnava, S., Barati, M.R. and Hamouda, A.M.S. (2020b), "Nonlinear dynamic characteristics of nonlocal multi-phase magneto-electro-elastic nano-tubes with different piezoelectric constituents", *Appl. Phys. A*, **126**(8), 605. https://doi.org/10.1007/s00339-020-03743-8.

Mirjavadi, S.S., Forsat, M., Barati, M.R. and Hamouda, A. (2020c), "Investigating nonlinear vibrations of multi-scale truncated conical shell segments with carbon nanotube/ fiberglass reinforcement using a higher order conical shell theory", *J. Strain Anal. Eng. Des*., **56**(3), 181-192. https://doi.org/10.1177/0309324720939811.

Mirjavadi, S.S., Forsat, M., Barati, M.R. and Hamouda, A.M.S. (2022), "Geometrically nonlinear vibration analysis of eccentrically stiffened porous functionally graded annular spherical shell segments", *Mech. Based Des. Struct*., **50**(6), 2206-2220. https://doi.org/10.1080/15397734.2020.1771729.

Mirjavadi, S.S., Khan, I., Forsat, M., Barati, M.R. and Hamouda, A.M.S. (2023), "Analyzing nonlinear vibration of metal foam stiffened toroidal convex/concave shell segments considering porosity distribution", *Mech. Based Des. Struct*., **51**(1), 310-326. https://doi.org/10.1080/15397734.2020.1841654.

Mirjavadi, S.S., Yahya, Y.Z., Forsat, M., Khan, I., Hamouda, A.M.S. and Barati, M.R. (2020d), "Magneto-electric effects on nonlocal nonlinear dynamic characteristics of imperfect multi-phase magneto-electro-elastic beams", *J. Magn. Magn. Mater*., **503** 166649. https://doi.org/10.1016/j.jmmm.2020.166649.

Mousavi, S.M., Shafiei, N. and Dadvand, A. (2017), "Numerical simulation of subsonic turbulent flow over NACA0012 airfoil: evaluation of turbulence models", *Sigma J. Eng. Natural Sci*., **35**(1), 133-155.

Omidi, S., Oskooee, M.B. and Shafiei, N. (2013), "Finite element analysis of an ultra-fine grained Titanium dental implant covered by different thicknesses of hydroxyapatite layer", *Indian J. Dent*., **4**(1), 1-4. https://doi.org/10.1016/j.ijd.2012.10.002.

Qi, L., Wang, Z., Sun, Y., Khorami, M., Mahmoudi, T. and Wu, H. (2024), "Modified couple stress and artificial intelligence examination of nonlinear buckling in porous variable thickness cylinder micro sport structures", *Mech. Adv. Mater. Struct*., 1-19. https://doi.org/10.1080/15376494.2024.2316795.

Rajasekaran, S., Khaniki, H.B. and Ghayesh, M.H. (2022), "Thermo-mechanics of multi-directional functionally graded elastic sandwich plates", *Thin Wall. Struct*., **176**, 109266. https://doi.org/10.1016/j.tws.2022.109266.

Shahabinejad, E., Shafiei, N. and Ghadiri, M. (2018), "Influence of temperature change on modal analysis of rotary functionally graded nano-beam in thermal environment", *J. Solid Mech*., **10**(4), 779-803. https://jsm.arak.iau.ir/article_545719.html.

Shan, X. and Huang, A. (2022), "Intelligent simulation of the thermal buckling characteristics of a tapered functionally graded porosity-dependent rectangular small-scale beam", *Adv. Nano Res*., **12**(3), 281-290. https://doi.org/10.12989/anr.2022.12.3.281.

Shi, X., Li, J. and Habibi, M. (2022), "On the statics and dynamics of an electro-thermo-mechanically porous GPLRC nanoshell conveying fluid flow", *Mech. Based Des. Struct*., **50**(6), 2147-2183. https://doi.org/10.1080/15397734.2020.1772088.

Song, G., Zou, Y., Nie, Y., Habibi, M., Albaijan, I. and Toghroli, E. (2024), "Application of Hashin–Shtrikman bounds homogenization

model for frequency analysis of imperfect FG bio-composite plates", *J. Mech. Behav. Biomed. Mater.*, **151**, 106321. https://doi.org/10.1016/j.jmbbm.2023.106321.

Song, S., Zhang, T. and Zhui, Z. (2023), "Dynamic analysis of nanotube-based nanodevices for drug delivery in sports-induced varied conditions applying the modified theories", *Steel Compos. Struct.*, **49**(5), 487. https://doi.org/10.12989/scs.2023.49.5.487.

Verheij, D., Peres, M., Cardoso, S., Alves, L.C., Alves, E., Durand, C., Eymery, J., Fernandes, J. and Lorenz, K. (2021), "Self-powered proton detectors based on GaN core–shell p–n microwires", *Appl. Phys. Lett.*, **118**(19), 193501. https://doi.org/10.1063/5.0045050.

Vollrath, F. and Knight, D.P. (2001), "Liquid crystalline spinning of spider silk", *Nature*, **410**(6828), 541-548. https://doi.org/10.1038/35069000.

Wang, B., Wang, Z., Song, Y., Zong, W., Zhang, L., Ji, K., Manoonpong, P. and Dai, Z. (2023a), "A Neural Coordination Strategy for Attachment and Detachment of a Climbing Robot Inspired by Gecko Locomotion", *Cyborg Bionic Syst.*, **4**, 0008. https://doi.org/10.34133/cbsystems.0008.

Wang, C., Habibi, M. and Mahmoudi, T. (2024a), "Stability analysis of the nonuniform functionally graded cylindrical small-scale beam structures: Application in sport structures", *Steel Compos. Struct.*, **52**(1), 15-29. https://doi.org/10.12989/scs.2024.52.1.015.

Wang, D., Bai, Y., Habibi, M. and Mahmoudi, T. (2024b), "Stability behaviors and governing equations of the volleyball game ball via GDQ and analytical methods", *Adv. Concr. Constr.*, **18**(6), 379. https://doi.org/10.12989/acc.2024.18.6.379.

Wang, D., Bai, Y., Habibi, M. and Mahmoudi, T. (2024c), "Stability behaviors and governing equations of the volleyball game ball via GDQ and analytical methods", *Adv. Concr. Constr.*, **18**(6), 379-388. https://doi.org/10.12989/acc.2024.18.6.379.

Wang, D., Feng, B., Liu, X., Habibi, M. and Mahmoudi, T. (2025), "Nanoparticle-infused oils for improved lubrication and wear resistance in internal combustion engines: Exploring nano-science applications in automotive parts", *Adv. Nano Res.*, **18**(1), 1. https://doi.org/10.12989/anr.2025.18.1.001

Wang, D., Wang, Q. and Habibi, M. (2024d), "Electro-magneto-elastic analysis of a sandwich composite beam as diving board in swimming with composed of graphene origami metamaterials", *Mech. Adv. Mater. Struct.*, 1-15. https://doi.org/10.1080/15376494.2024.2422579.

Wang, F., Gao, S., Habibi, M. and Luo, Z. (2024e), "Energy absorption of vibrating sport equipment used for testing athlete performance", *Adv. Nano Res.*, **17**(5), 421-434. https://doi.org/10.12989/anr.2024.17.5.421.

Wang, G., Peng, K., Zhou, H., Liu, G., Lou, Z. and Pan, F. (2023b), "Nanocomposite reinforced structures to deal with injury in physical sports", *Adv. Nano Res.*, **14**(6), 541-555. https://doi.org/10.12989/anr.2023.14.6.541.

Wang, J., Chen, Y. and Zou, Q. (2023c), "Inferring gene regulatory network from single-cell transcriptomes with graph autoencoder model", *PLOS Genetics*, **19**(9), e1010942. https://doi.org/10.1371/journal.pgen.1010942.

Wang, L., Habibi, M. and Huang, G. (2024f), "Smart analysis of sandwich foldable cylinders as gymnastic accessories", *Mech. Adv. Mater. Struct.*, 1-18. https://doi.org/10.1080/15376494.2024.2411414.

Wang, N., Zhang, T., Yang, J., Habibi, M. and Feng, J. (2024g), "Electro-magneto-mechanical critical load analysis of piezo-electric/piezomagnetic sport force plates used for testing athlete performance", *Mech. Adv. Mater. Struct.*, 1-15. https://doi.org/10.1080/15376494.2024.2414944.

Wang, P., Gao, Z., Pan, F., Moradi, Z., Mahmoudi, T. and Khadimallah, M.A. (2022), "A couple of GDQM and iteration techniques for the linear and nonlinear buckling of bi-directional functionally graded nanotubes based on the nonlocal strain gradient theory and high-order beam theory", *Eng. Anal. Bound. Elem.*, **143**, 124-136. https://doi.org/10.1016/j.enganabound.2022.06.007.

Wang, T., Niu, B., Xu, N. and Zhang, L. (2024h), "ADP-based online compensation hierarchical sliding-mode control for partially unknown switched nonlinear systems with actuator failures", *ISA Transactions*, **155**, 69-81. https://doi.org/10.1016/j.isatra.2024.09.011.

Wang, W., Zhang, J., Habibi, M. and Albaijan, I. (2024i), "Stretchable-thickness model for dynamic responses of graphene origami reinforced badminton sport plate", *Mech. Adv. Mater. Struct.*, 1-13. https://doi.org/10.1080/15376494.2024.2373976.

Wang, Y., Zhai, Y., Ding, Y. and Zou, Q. (2024j), "SBSM-Pro: support bio-sequence machine for proteins", *Sci. China Inform. Sci.*, **67**(11), 212106. https://doi.org/10.1007/s11432-024-4171-9.

Wang, Y., Zhang, X., Ju, Y., Liu, Q., Zou, Q., Zhang, Y., Ding, Y. and Zhang, Y. (2024k), "Identification of human microRNA-disease association via low-rank approximation-based link propagation and multiple kernel learning", *Front. Comput. Sci.*, **18**(2), 182903. https://doi.org/10.1007/s11704-023-2490-5.

Wu, Q., Zou, S., Liu, W., Liang, M., Chen, Y., Chang, J., Liu, Y. and Yu, X. (2023), "A novel onco-cardiological mouse model of lung cancer-induced cardiac dysfunction and its application in identifying potential roles of tRNA-derived small RNAs", *Biomed. Pharmacotherapy*, **165**, 115117. https://doi.org/10.1016/j.biopha.2023.115117.

Wu, W., Zhao, N., Zhang, L. and Wu, Y. (2024a), "Approximation-based adaptive two-bit-triggered bipartite tracking control for nonlinear networked MASs subject to periodic disturbances", *Robotic Intell. Autom.*, **44**(6), 791-805. https://doi.org/10.1108/RIA-01-2024-0026.

Wu, X., Ding, S., Wang, H., Xu, N., Zhao, X. and Wang, W. (2025), "Dual-channel event-triggered prescribed performance adaptive fuzzy time-varying formation tracking control for nonlinear multi-agent systems", *Fuzzy Sets Syst.*, **498**, 109140. https://doi.org/10.1016/j.fss.2024.109140.

Wu, Y., Liang, H., Zhao, N. and Niu, B. (2024b), "Low-computation-based adaptive self-triggered bipartite consensus control for nonlinear multiagent systems subject to sensor faults", *IEEE T Control Netw. Syst.*, **11**(4), 2114-2125. https://doi.org/10.1109/TCNS.2024.3373132.

Xiao, H., Habibi, M. and Habibi, M. (2024), "Bulk wave propagation analysis of imperfect FG bio-composite beams resting on variable elastic medium", *Mater. Today Commun.*, **39**, 108524. https://doi.org/10.1016/j.mtcomm.2024.108524.

Yan, C., Zhang, T., Zheng, T. and Mahmoudi, T. (2024), "Stability characteristic of bi-directional FG nano cylindrical imperfect composite: Improving the performance of sports bikes using carbon nanotubes", *Steel Compos. Struct.*, **50**(4), 459-474. https://doi.org/10.12989/scs.2024.50.4.459.

Yang, L., van der Werf, K.O., Fitié, C.F.C., Bennink, M.L., Dijkstra, P.J. and Feijen, J. (2008), "Mechanical Properties of Native and Cross-linked Type I Collagen Fibrils", *Biophys. J.*, **94**(6), 2204-2211. https://doi.org/10.1529/biophysj.107.111013.

Yi, W. (2022), "Intelligent computer modelling and simulation for the large amplitude of nano systems", *Adv. Nano Res.*, **13**(1), 63-75. https://doi.org/10.12989/anr.2022.13.1.063.

Yu, C., Lin, P., Wu, Z., Habibi, M. and Zhang, W. (2024), "Multi-load effect on the deformation analysis of composite nano reinforced origami sandwich panel", *Mech. Adv. Mater. Struct.*, 1-19. https://doi.org/10.1080/15376494.2024.2367015.

Zhang, D., Huang, X., Wang, T., Habibi, M., Albaijan, I. and

Toghroli, E. (2024a), "Dynamic stability improvement in spinning FG-piezo cylindrical structure using PSO-ANN and firefly optimization algorithm", *Mater. Sci. Eng. B*, **302**, 117210. https://doi.org/10.1016/j.mseb.2024.117210.

Zhang, H., Habibi, M. and Zou, Y. (2024b), "Static analysis of foldable pressurized and thermally loaded cylindrical shell as an expander in sport equipment reinforced by G-Ori nanofillers", *Mech. Adv. Mater. Struct.*, 1-13. https://doi.org/10.1080/15376494.2024.2412307.

Zhang, P., Song, J. and Mahmoudi, T. (2023a), "Simulation and modeling for stability analysis of functionally graded non-uniform pipes with porosity-dependent properties", *Steel Compos. Struct.*, **48**(2), 235-250. https://doi.org/10.12989/scs.2023.48.2.235.

Zhang, X., Li, J., Cui, Y., Habibi, M., Ali, H.E., Albaijan, I. and Mahmoudi, T. (2023b), "Static analysis of 2D-FG nonlocal porous tube using gradient strain theory and based on the first and higher-order beam theory", *Steel Compos. Struct.*, **49**(3), 293-306. https://doi.org/10.12989/scs.2023.49.3.293.

Zhang, Z., Du, J. and Mahmoudi, T. (2023c), "Green synthesis of silver nanoparticles to the microbiological corrosion deterrence of oil and gas pipelines buried in the soil", *Adv. Nano Res.*, **15**(4), 355-366. https://doi.org/10.12989/anr.2023.15.4.355.

Zhao, J., Wan, L., Habibi, M. and Brahmia, A. (2024), "An adaptive neuro-fuzzy approach using IoT data in predicting springback in ultra-thin stainless steel sheets with consideration of grain size", *Adv. Nano Res.*, **17**(2), 109. https://doi.org/10.12989/.2024.17.2.109.

Zhiqiang, S., Aiyun, L., Daichang, Z., Shuangjun, L., Habibi, M., Xiaoling, F. and Albaijan, I. (2024), "Application of a folded nanostructure reinforcement for the pole vault curved shell", *Mech. Adv. Mater. Struct.*, 1-15. https://doi.org/10.1080/15376494.2024.2375368.

Zhou, W., Huang, Y., Wu, Z., Habibi, M., Habibi, M. and Marzouki, R. (2025), "Influence of agglomeration and waviness phenomena on torsional oscillation of MWCNTs-reinforced composite rods", *Int. J. Solids Struct.*, **306**, 113127. https://doi.org/10.1016/j.ijsolstr.2024.113127.

Zhu, J., Wang, Y., An, N., Habibi, M. and Wang, H. (2024a), "Application of G-Ori metamaterials as sports equipment baseball bat in an electro-magneto-elastic sandwich composite beam", *Mech. Adv. Mater. Struct.*, 1-20. https://doi.org/10.1080/15376494.2024.2414198.

Zhu, K., Ma, W., Dong, J., Chen, M., Habibi, M. and Albaijan, I. (2024b), "On the dispersion of bulk wave in hygrothermally affected poroelastic gymnastics beams based on refined higher-order shear deformation theory during athlete training", *Mech. Adv. Mater. Struct.*, 1-10. https://doi.org/10.1080/15376494.2024.2428830.

Zhu, L., Ren, H., Habibi, M., Mohammed, K.J. and Khadimallah, M.A. (2022), "Predicting the environmental economic dispatch problem for reducing waste nonrenewable materials via an innovative constraint multi-objective Chimp Optimization Algorithm", *J. Clean. Prod.*, **365**, 132697. https://doi.org/10.1016/j.jclepro.2022.132697.

Zisong, Z. and Habibi, M. (2024), "AI-assisted prediction of St14 steel sheets formability: Neural-fuzzy systems and crystal plasticity assessments", *Structures*, **65**, 106633. https://doi.org/10.1016/j.istruc.2024.106633.